Topological Nature of the Phonon Hall Effect

Lifa Zhang,[1] Jie Ren,[2,1] Jian-Sheng Wang,[1] and Baowen Li[2,1]

[1]*Department of Physics and Centre for Computational Science and Engineering, National University of Singapore, Singapore 117542, Republic of Singapore*

[2]*NUS Graduate School for Integrative Sciences and Engineering, Singapore 117456, Republic of Singapore*

(Received 2 August 2010; published 24 November 2010)

We provide a topological understanding of the phonon Hall effect in dielectrics with Raman spin-phonon coupling. A general expression for phonon Hall conductivity is obtained in terms of the Berry curvature of band structures. We find a nonmonotonic behavior of phonon Hall conductivity as a function of the magnetic field. Moreover, we observe a phase transition in the phonon Hall effect, which corresponds to the sudden change of band topology, characterized by the altering of integer Chern numbers. This can be explained by touching and splitting of phonon bands.

DOI: 10.1103/PhysRevLett.105.225901 PACS numbers: 66.70.−f, 03.65.Vf, 72.10.Bg, 72.15.Gd

Recent years have witnessed a rapid development of an emerging field—phononics, the science and technology of controlling heat flow and processing information with phonons [1]. Indeed, in parallel with electronics, various functional thermal devices such as thermal diodes [2], thermal transistors [3], thermal logic gates [4], and thermal memory [5], etc., have been proposed to manipulate and control phonons, the carriers of heat energy and information. However, different from electrons, phonons as neutral quasiparticles cannot directly couple to the magnetic field through the Lorentz force. Therefore, it is a surprise that Strohm, Rikken, and Wyder observed the phonon Hall effect (PHE)—the appearance of a temperature difference in the direction perpendicular to both the applied magnetic field and the heat current flowing through an ionic paramagnetic dielectric sample [6]. It was confirmed later by Inyushkin and Taldenkov [7]. Since then, several theoretical explanations have been proposed [8–10] to understand this novel phenomenon.

For electronic transport properties in various quantum, spin, or anomalous Hall effects [11–13], topological Berry phase has been successfully used to understand the underlying mechanism [14]. Such an elegant connection between mathematics and physics provides a broad and deep understanding of basic material properties. However, because of the very different nature of electrons and phonons, a topological picture related to the PHE is not straightforward and obvious and, therefore, is still lacking.

In this Letter, we explore the topology of phonon bands in a two-dimensional honeycomb lattice with Raman-type spin-phonon interaction. A general expression for phonon Hall conductivity in terms of Berry curvature is derived. The phonon Hall effect is not quantized, although the Chern numbers are quantized to integers. We find that there exists a phase transition associated with the PHE, due to the discontinuous jump of Chern numbers.

We start with a Hamiltonian for an ionic crystal lattice in a uniform external magnetic field [15], which reads in a compact form as

$$H = \tfrac{1}{2}(p - \tilde{A}u)^T(p - \tilde{A}u) + \tfrac{1}{2}u^T K u = \tfrac{1}{2}p^T p + \tfrac{1}{2}u^T(K - \tilde{A}^2)u + u^T\tilde{A}p. \quad (1)$$

Here, u is a column vector of displacements from lattice equilibrium positions for all the degrees of freedom, multiplied by the square root of mass, p is the conjugate momentum vector, and K is the force constant matrix. The superscript T stands for the matrix transpose. $\tilde{A}$ is an antisymmetric real matrix, which is block diagonal with elements

$$\Lambda = \begin{pmatrix} 0 & h \\ -h & 0 \end{pmatrix}$$

(in two dimensions), where h is proportional to the magnitude of the applied magnetic field and has the dimension of frequency. For simplicity, we will call h the magnetic field later. The on-site term $u^T\tilde{A}p$ can be interpreted as the Raman (or spin-phonon) interaction [16]. The Hamiltonian (1) is positive definite.

By applying Bloch's theorem, we can describe the system by the polarization vector $x = (\mu, \epsilon)^T$, where μ and ϵ are associated with the momenta and coordinates, respectively. The equation of motion can be expressed as

$$i\frac{\partial}{\partial t}x = H_{\text{eff}}x, \qquad H_{\text{eff}} = i\begin{pmatrix} -A & -D \\ I & -A \end{pmatrix}, \quad (2)$$

where $D(\mathbf{k}) = -A^2 + \sum_{l'} K_{l,l'} e^{i(\mathbf{R}_{l'} - \mathbf{R}_l)\cdot\mathbf{k}}$ is the dynamic matrix as a function of wave vector $\mathbf{k}$, $K_{l,l'}$ is the submatrix between unit cell l and l' in the full spring constant matrix K, $\mathbf{R}_l$ is the real-space lattice vector, A is block diagonal with elements Λ, and I is an identity matrix. Here, D, A, $K_{l,l'}$, and I are all 4×4 matrices for the two-dimensional honeycomb lattice. The eigenvalue problem of the equation of motion (2) reads

$$H_{\rm eff}x_\sigma = \omega_\sigma x_\sigma, \tag{3}$$

where $x_\sigma = (\mu_\sigma, \epsilon_\sigma)^T$ is the right eigenvector of the σth branch and ω_σ is the corresponding eigenfrequency. Because of the non-Hermitian nature of $H_{\rm eff}$, the left eigenvector is different and is given by $\tilde{x}_\sigma^T = (\tilde{\mu}_\sigma, \tilde{\epsilon}_\sigma) = (\epsilon_\sigma^\dagger, -\mu_\sigma^\dagger)/(-2i\omega_\sigma)$. The orthonormal condition is $\epsilon_\sigma^\dagger \epsilon_{\sigma'} + \frac{i}{\omega_\sigma}\epsilon_\sigma^\dagger A \epsilon_{\sigma'} = \delta_{\sigma,\sigma'}$ [10].

By taking into account only positive eigenfrequency modes, displacement and momentum operators can be written in the second quantization form. From the definition of energy current density $\mathbf{J} = \frac{1}{2V}\sum_{l,l'}(\mathbf{R}_l - \mathbf{R}_{l'})u_l^T K_{l,l'}\dot{u}_{l'}$ [8,9,17], the current density vector can be expressed as

$$\mathbf{J} = \mathbf{J_1}(a^\dagger a) + \mathbf{J_2}(a^\dagger a^\dagger, aa). \tag{4}$$

Here, $\mathbf{J_1} = \frac{\hbar}{4V}\sum_{k,k'}[(\omega_k + \omega_{k'})/\sqrt{\omega_k\omega_{k'}}]\epsilon_k^\dagger \frac{\partial D(\mathbf{k})}{\partial \mathbf{k}}\epsilon_{k'} a_k^\dagger a_{k'} e^{i(\omega_k - \omega_{k'})t}\delta_{\mathbf{k},\mathbf{k}'}$ and $\mathbf{J_2} = \frac{\hbar}{4V}\sum_{k,k'}\sqrt{\omega_{k'}/\omega_k}(\epsilon_k^\dagger \frac{\partial D(\mathbf{k})}{\partial \mathbf{k}}\epsilon_{k'}^* a_k^\dagger a_{k'}^\dagger e^{i(\omega_k + \omega_{k'})t} + \epsilon_k^T \frac{\partial D^*(\mathbf{k})}{\partial \mathbf{k}}\epsilon_{k'} a_k a_{k'} e^{-i(\omega_k + \omega_{k'})t})\delta_{\mathbf{k},-\mathbf{k}'}$, where $k = (\mathbf{k}, \sigma)$ considers both the wave vector and the phonon branch. It should be noted that the $a^\dagger a^\dagger$ and aa terms also contribute to the off-diagonal elements of thermal conductivity tensor, although they have no contribution to the average heat flux. The diagonal term $\epsilon_k^\dagger \frac{\partial D(\mathbf{k})}{\partial \mathbf{k}}\epsilon_k$ in $\mathbf{J_1}$ corresponds to $\omega_\sigma \frac{\partial \omega_\sigma}{\partial \mathbf{k}}$. Only the off-diagonal terms in $\mathbf{J_1}$ and $\mathbf{J_2}$ contribute to the Hall conductivity, which can be regarded as the contribution from anomalous velocities similar to the one in the intrinsic anomalous Hall effect [12]. Using the Green-Kubo formula $\kappa_{xy} = \frac{V}{\hbar T}\times \int_0^{\beta\hbar} d\lambda \int_0^\infty dt \langle J^x(-i\lambda)J^y(t)\rangle_{\rm eq}$ [18], one can obtain phonon Hall conductivity as [16]

$$\kappa_{xy} = \frac{\hbar}{8VT}\sum_{\sigma\neq\sigma'} f(\omega_\sigma)(\omega_\sigma + \omega_{\sigma'})^2 \frac{i}{4\omega_\sigma\omega_{\sigma'}} \times \frac{\epsilon_\sigma^\dagger \frac{\partial D}{\partial k_x}\epsilon_{\sigma'}\epsilon_{\sigma'}^\dagger \frac{\partial D}{\partial k_y}\epsilon_\sigma - (k_x \leftrightarrow k_y)}{(\omega_\sigma - \omega_{\sigma'})^2}, \tag{5}$$

where $f(\omega_\sigma) = (e^{\hbar\omega_\sigma/(k_B T)} - 1)^{-1}$ is the Bose distribution function, V is the total volume of the sample, and the phonon branch index σ here includes both the positive and negative eigenvalues without restrictions. It can be proved that the phonon Hall conductivity κ_{xy} satisfies the Onsager reciprocal relations [16].

In Fig. 1, we show the phonon Hall conductivity of honeycomb lattices calculated from Eq. (5). The parameters used in our numerical calculations are the same as in Ref. [10]. The coupling matrix between two sites is configured such that the longitudinal spring constant is $K_L = 0.144\ \mathrm{eV/(u\,\AA^2)}$ and the transverse one K_T is 4 times smaller. The unit cell lattice vectors are $(a, 0)$ and $(a/2, a\sqrt{3}/2)$ with $a = 1$ Å.

It is found that when h is small, κ_{xy} is proportional to h [16], while the dependence becomes nonlinear when h is large. As h is further increased, κ_{xy} increases before it reaches a maximum at a certain value of h. Then κ_{xy} decreases and goes to zero at very large h. This can be understood as follows: Numerical calculation shows that $\omega_\sigma \approx \alpha h$, which can also be obtained from the equation $[(-i\omega_\sigma + A)^2 + D]\epsilon_\sigma = 0$ [16]; thus, we can obtain approximately $\kappa_{xy} \sim h^2/(e^{\beta\hbar\alpha h} - 1)$ from Eq. (5). In the weak magnetic field limit $\kappa_{xy} \propto h$, while in the strong field limit $\kappa_{xy} \to 0$. The on-site term $\tilde{A}^2$ in the Hamiltonian (1) increases with h quadratically so as to blockade the phonon transport, which competes with the spin-phonon interaction. Therefore, as h increases, κ_{xy} first increases, then decreases, and tends to zero at last. At low temperatures, κ_{xy} oscillates around zero with the variation of h, as shown in the inset in Fig. 1(a).

There is a subtle singularity near $h \simeq 25$ rad/ps in Fig. 1(a); we thus plot the first derivative of κ_{xy} with respect to h at different temperatures in Fig. 1(b). It shows that, at the relatively high temperatures, the first derivative of phonon Hall conductivity has a minimum at the magnetic field $h_c \simeq 25.4778$ rad/ps for the finite-size sample $N_L = 400$ (the sample has $N = N_L^2$ unit cells). The first derivative $d\kappa_{xy}/dh$ at the point h_c diverges when the system size increases to infinity. The inset in Fig. 1(b) shows the finite-size effect. At the point h_c, the second derivative $d^2\kappa_{xy}/dh^2$ is discontinuous. Therefore, h_c is a critical point for the PHE, across which a phase transition occurs. At low temperatures, the divergence of $d\kappa_{xy}/dh$ is not so evident as that at high temperatures. However, if the sample size becomes larger, the discontinuity of $d^2\kappa_{xy}/dh^2$ is more obvious, as illustrated in Fig. 1(b). For different temperatures, the phase transition occurs at exactly the

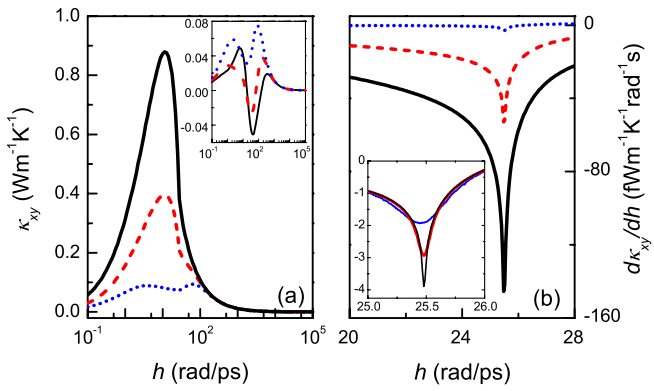

FIG. 1 (color online). (a) Phonon Hall conductivity vs magnetic field for different temperatures. The dotted, dashed, and solid lines correspond to $T = 50$, 100, and 300 K, respectively. The inset shows h dependence of κ_{xy} at low temperatures: $T = 10$ (solid line), 20 (dashed line), and 40 K (dotted line). (b) $d\kappa_{xy}/dh$ as a function of h at different temperatures: $T = 50$ (dotted line), 100 (dashed line), and 300 K (solid line); here $N_L = 400$. The inset in (b) shows the h dependence of $d\kappa_{xy}/dh$ for different sizes N_L at $T = 50$ K, around $h \approx 25.5$ rad/ps; from top to bottom, $N_L = 80$, 320, and 1280, respectively.

same critical value h_c, which strongly suggests that the phase transition of the PHE is related to the topology of the phonon band structure.

In the following, we would like to connect the PHE with the Berry phase to examine the underlying topological mechanism. As is well known, the band structure of crystals provides a natural platform to investigate the geometric phase effect. Since the wave-vector dependence of the polarization vectors is inherent to the Hall problems, the Berry phase effects are intuitively expected for the PHE in the momentum space. Following Berry's approach [14], we set $x(t) = e^{i\gamma_\sigma(t) - i\int_0^t dt' \omega_\sigma[\mathbf{k}(t')]} x_\sigma[\mathbf{k}(t)]$ and then insert it into Eq. (2). The Berry phase is obtained as $\gamma_\sigma = \oint \mathbf{A}^\sigma_{\mathbf{k}} \cdot d\mathbf{k}$, with $\mathbf{A}^\sigma_{\mathbf{k}} = i\tilde{x}^T_\sigma \frac{\partial x_\sigma}{\partial \mathbf{k}}$, and the Berry curvature emerges as

$$\Omega^\sigma_{k_x k_y} = \frac{\partial}{\partial k_x}\mathbf{A}^\sigma_{k_y} - \frac{\partial}{\partial k_y}\mathbf{A}^\sigma_{k_x} = \sum_{\sigma',\sigma'\neq\sigma} \Omega^{\sigma\sigma'}_{k_x k_y}, \tag{6}$$

where

$$\Omega^{\sigma\sigma'}_{k_x k_y} = \frac{i}{4\omega_\sigma\omega_{\sigma'}} \frac{\epsilon^\dagger_\sigma \frac{\partial D}{\partial k_x}\epsilon_{\sigma'}\epsilon^\dagger_{\sigma'}\frac{\partial D}{\partial k_y}\epsilon_\sigma - \epsilon^\dagger_\sigma \frac{\partial D}{\partial k_y}\epsilon_{\sigma'}\epsilon^\dagger_{\sigma'}\frac{\partial D}{\partial k_x}\epsilon_\sigma}{(\omega_\sigma - \omega_{\sigma'})^2} \tag{7}$$

is the contribution to the Berry curvature of the band σ from a different band σ'. The associated topological Chern number is obtained through integrating the Berry curvature over the first Brillouin zone as

$$C^\sigma = \frac{1}{2\pi}\int_{\mathrm{BZ}} dk_x dk_y \Omega^\sigma_{k_x k_y} = \frac{2\pi}{L^2}\sum_{\mathbf{k}} \Omega^\sigma_{k_x k_y}, \tag{8}$$

where L is the length of the sample. The phonon Hall conductivity formula [Eq. (5)] is recast into

$$\kappa_{xy} = \frac{\hbar}{8VT}\sum_{\mathbf{k},\sigma\neq\sigma'} f(\omega_\sigma)(\omega_\sigma + \omega_{\sigma'})^2 \Omega^{\sigma\sigma'}_{k_x k_y}. \tag{9}$$

Here $V = L^2 a$. The term $(\omega_\sigma + \omega_{\sigma'})^2$ relating to the phonon energy is an analog of the electrical charge term e^2 in the electron Hall effect; thus, the phonon Hall conductivity [Eq. (9)] is similar to but different from the electron case because the phonon energy term cannot be moved out from the summation. Although the formula is derived from the phonon transport in the crystal-lattice system, we note that the thermal Hall conductivity for the magnon Hall effect [19] can also be cast into the form of Eq. (9) with a different expression for the Berry curvature. Therefore, the Hall conductivity formula can be universally applicable to the thermal Hall effect in phonon and magnon systems without restriction for special lattice structures.

Without the Raman spin-phonon interaction, namely, $h = 0$, $\Omega^{\sigma\sigma'}_{k_x k_y}$ is zero everywhere and the phonon Hall conductivity vanishes. When a magnetic field is applied, the Berry curvature is nonzero, and, consequently, the PHE appears. It is found that if the system exhibits symmetry satisfying $SDS^{-1} = D$, $SAS^{-1} = -A$ (e.g., mirror reflection symmetry), the phonon Hall conductivity is zero [10,16]. This symmetry principle can also be applied to the topological property of the phonon bands: We find that $\Omega^{\sigma\sigma'}_{k_x k_y} = 0$ provided that such symmetry exists, such as in the square lattice system, whereas if such symmetry is broken for the dynamic matrix, the system can possess nontrivial Berry curvatures. In the system with the PHE, if the magnetic field changes, the Berry curvatures are quite different. However, we find that the associated topological Chern numbers remain constant integers with occasional jumps when h is varied. Therefore, the Chern numbers given by Eq. (8) are topological invariant, which indeed illustrates the nontrivial topology of the phonon band structures. Although the Chern numbers are quantized to integers, the phonon Hall conductivity is not, due to the extra term $f(\omega_\sigma)(\omega_\sigma + \omega_{\sigma'})^2$. Thus, the analogy to the quantum Hall effect is incomplete.

In the vicinity of the critical magnetic field h_c, we find that the phase transition is indeed related to the abrupt change of the topology of band structures. The Berry curvatures for different bands near the critical magnetic field are illustrated in Figs. 2(a)–2(f) and 2(h). We find that, with an infinitesimal change of magnetic field around h_c, the Berry curvatures around the Γ ($\mathbf{k} = 0$) point of bands 2 and 3 are quite different, whereas those of bands 1 and 4 remain unchanged. To illustrate the change of the Berry curvatures clearly, we plot the cross section of the Berry curvatures along the k_x direction for bands 2 and 3 in Fig. 2(i), which shows explicitly that the Berry curvatures change dramatically above and below the critical magnetic field h_c. Below the critical point, the Berry curvature for band 2 in the vicinity of Γ point contributes Berry phase 2π (-2π for band 3), which cancels that from K and K' points, so that the Chern number is zero for bands 2 and 3, as indicated in Fig. 2(j). However, above the critical point, the sum of Berry curvature at Γ point is zero, and only the monopole at K and K' points contributes to Berry phase (-2π for band 2 and 2π for band 3). Therefore, the Chern numbers jump from 0 to ± 1, as shown in Fig. 2(j). This jump indicates that the topology of the two bands suddenly changes at the critical magnetic field, which is responsible for the phase transition. From a calculation on the kagome lattice, which has been used to model many real materials [20], we also find qualitatively similar phase transitions due to the sudden change of topology, where the phonon Hall conductivity has three singularities of divergent first derivatives corresponding to three jumps of the Chern numbers.

To further investigate the mechanism of the abrupt change of the phonon band topology, we study the dispersion relation near the critical magnetic field. From Fig. 2(k), we can see that bands 2 and 3 are going to touch with each other at the Γ point if the magnetic field increases to h_c; at the critical magnetic field, the degeneracy occurs and the two bands possess the cone shape; above the critical point h_c, the two bands split up. Therefore, the difference between the two bands decreases below and increases above the critical point h_c. The property of the dispersion relation

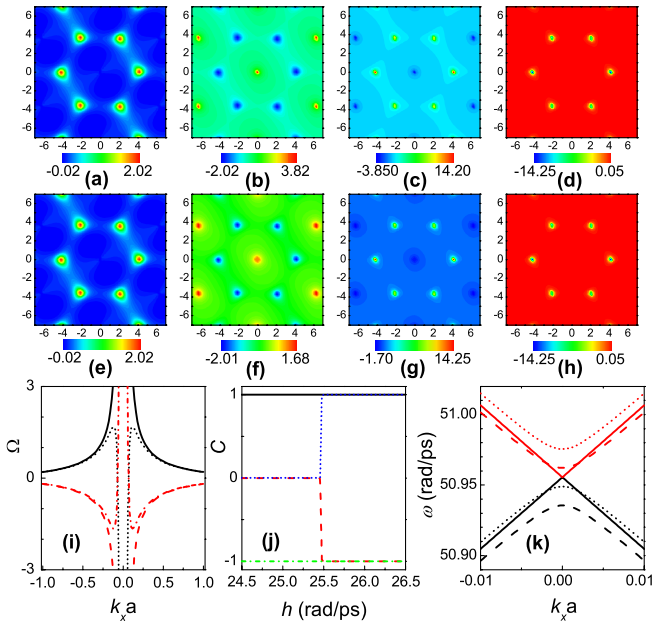

FIG. 2 (color online). (a)–(d) The contour map of Berry curvatures for bands 1–4 at $h_{c-} = h_c - 10^{-2}$ rad/ps; (e)–(h) The contour map of Berry curvatures for bands 1–4 at $h_{c+} = h_c + 10^{-2}$ rad/ps. For (a)–(h), the horizontal and vertical axes correspond to wave vector k_x and k_y, respectively. (i) Ω at different magnetic fields. The solid and dashed lines correspond to Ω^2 and Ω^3 at h_{c-}, respectively, while dotted and dash-dotted lines correspond to those at h_{c+}. (j) Chern numbers of four bands: C^1 (solid line), C^2 (dashed line), C^3 (dotted line), and C^4 (dash-dotted line). (k) The dispersion relation of bands 2 and 3 at different magnetic fields in the vicinity of h_c. The dashed, solid, and dotted lines correspond to the bands at h_{c-}, h_c, and h_{c+}, respectively. The lower three and upper three correspond to bands 2 and 3, respectively. $k_y = 0$ in (i) and (k).

in the vicinity of the critical magnetic field directly affects the Berry curvature of the corresponding bands.

In summary, we have studied the PHE from a topological point of view. By looking at the phases of the polarization vectors of both the displacements and conjugate momenta as a function of the wave vector, a Berry curvature can be defined uniquely for each band. This Berry curvature can be used to calculate the phonon Hall conductivity. Because of the nature of phonons, the phonon Hall conductivity, which is not directly proportional to the Chern number, is not quantized. However, the quantization effect, in the sense of discontinuous jumps in Chern numbers, manifests itself in the phonon Hall conductivity as a singularity of the first derivative with respect to the magnetic field.

The topological approach for phonon Hall conductivity proposed here is general and can be applied to real materials in low temperatures where the thermal transport is ballistic. It can also be applied to the magnon Hall effect discovered recently [19]. Phase transition in the PHE, explained from topological nature and dispersion relations, can also be generalized to study the phase transition in other Hall effects and/or nonequilibrium transport. In line with recently reported Berry-phase-induced heat pumping [21] and the Berry-phase contribution of molecular vibrational instability [22], we hope our present results do invigorate the studies aimed at uncovering intriguing Berry phase effects and topological properties in phonon transport, which will enrich further the discipline of phononics.

L. Z. thanks Bijay Kumar Agarwalla and Jie Chen for fruitful discussions. This project is supported in part by Grants No. R-144-000-257-112 and No. R-144-000-222-646 of NUS.

[1] L. Wang and B. Li, Phys. World **21**, 27 (2008).
[2] B. Li, L. Wang, and G. Casati, Phys. Rev. Lett. **93**, 184301 (2004); C. W. Chang, D. Okawa, A. Majumdar, and A. Zettl, Science **314**, 1121 (2006).
[3] B. Li, L. Wang, and G. Casati, Appl. Phys. Lett. **88**, 143501 (2006).
[4] L. Wang and B. Li, Phys. Rev. Lett. **99**, 177208 (2007).
[5] L. Wang and B. Li, Phys. Rev. Lett. **101**, 267203 (2008).
[6] C. Strohm, G. L. J. A. Rikken, and P. Wyder, Phys. Rev. Lett. **95**, 155901 (2005).
[7] A. V. Inyushkin and A. N. Taldenkov, JETP Lett. **86**, 379 (2007).
[8] L. Sheng, D. N. Sheng, and C. S. Ting, Phys. Rev. Lett. **96**, 155901 (2006).
[9] Y. Kagan and L. A. Maksimov, Phys. Rev. Lett. **100**, 145902 (2008).
[10] J.-S. Wang and L. Zhang, Phys. Rev. B **80**, 012301 (2009); L. Zhang, J.-S. Wang, and B. Li, New J. Phys. **11**, 113038 (2009).
[11] D. J. Thouless, M. Kohmoto, M. P. Nightingale, and M. den Nijs, Phys. Rev. Lett. **49**, 405 (1982).
[12] N. Nagaosa, J. Sinova, S. Onoda, A. H. MacDonald, and N. P. Ong, Rev. Mod. Phys. **82**, 1539 (2010).
[13] M. Koenig *et al.*, J. Phys. Soc. Jpn. **77**, 031007 (2008).
[14] D. Xiao, M.-C. Chang, and Q. Niu, Rev. Mod. Phys. **82**, 1959 (2010).
[15] A. Holz, Nuovo Cimento Soc. Ital. Fis. B **9**, 83 (1972).
[16] See the supplementary material at http://link.aps.org/supplemental/10.1103/PhysRevLett.105.225901 for detailed discussion.
[17] R. J. Hardy, Phys. Rev. **132**, 168 (1963).
[18] G. D. Mahan, *Many-Particle Physics* (Kluwer Academic, New York, 2000), 3rd ed.
[19] H. Katsura, N. Nagaosa, and P. A. Lee, Phys. Rev. Lett. **104**, 066403 (2010); Y. Onose, T. Ideue, H. Katsura, Y. Shiomi, N. Nagaosa, and Y. Tokura, Science **329**, 297 (2010).
[20] I. Syozi, Prog. Theor. Phys. **6**, 306 (1951); M. Takano, T. Shinjo, M. Kiyama, and T. Takada, J. Phys. Soc. Jpn. **25**, 902 (1968); M. Wolf and K. D. Schotte, J. Phys. A **21**, 2195 (1988); V. Elser, Phys. Rev. Lett. **62**, 2405 (1989); C. Broholm, G. Appli, G. P. Espinosa, and A. S. Cooper, Phys. Rev. Lett. **65**, 3173 (1990).
[21] J. Ren, P. Hänggi, and B. Li, Phys. Rev. Lett. **104**, 170601 (2010).
[22] J.-T. Lü, M. Brandbyge, and P. Hedegård, Nano Lett. **10**, 1657 (2010).